Vanessa Pellegrinelli,[1,2] Christine Rouault,[1,2,3] Sergio Rodriguez-Cuenca,[4] Victorine Albert,[1,2,3] Frédérique Edom-Vovard,[5,6,7,8] Antonio Vidal-Puig,[4] Karine Clément,[1,2,3] Gillian S. Butler-Browne,[5,6,7,8] and Danièle Lacasa[1,2,3]

Human Adipocytes Induce Inflammation and Atrophy in Muscle Cells During Obesity

Diabetes 2015;64:3121–3134 | DOI: 10.2337/db14-0796

Inflammation and lipid accumulation are hallmarks of muscular pathologies resulting from metabolic diseases such as obesity and type 2 diabetes. During obesity, the hypertrophy of visceral adipose tissue (VAT) contributes to muscle dysfunction, particularly through the dysregulated production of adipokines. We have investigated the cross talk between human adipocytes and skeletal muscle cells to identify mechanisms linking adiposity and muscular dysfunctions. First, we demonstrated that the secretome of obese adipocytes decreased the expression of contractile proteins in myotubes, consequently inducing atrophy. Using a three-dimensional coculture of human myotubes and VAT adipocytes, we showed the decreased expression of genes corresponding to skeletal muscle contractility complex and myogenesis. We demonstrated an increased secretion by cocultured cells of cytokines and chemokines with interleukin (IL)-6 and IL-1β as key contributors. Moreover, we gathered evidence showing that obese subcutaneous adipocytes were less potent than VAT adipocytes in inducing these myotube dysfunctions. Interestingly, the atrophy induced by visceral adipocytes was corrected by IGF-II/insulin growth factor binding protein-5. Finally, we observed that the skeletal muscle of obese mice displayed decreased expression of muscular markers in correlation with VAT hypertrophy and abnormal distribution of the muscle fiber size. In summary, we show the negative impact of obese adipocytes on muscle phenotype, which could contribute to muscle wasting associated with metabolic disorders.

During obesity, hypertrophy of white adipose tissue (WAT) is associated with fibro-inflammation and cell dysfunction. However, visceral depot (visceral adipose tissue [VAT]) differs from subcutaneous adipose tissue (SAT) by its inflammatory status because of its high infiltration with immune cells such as macrophages, T lymphocytes, and mast cells (1,2). Hence, VAT hypertrophy is considered an important contributor to obesity-related metabolic and cardiovascular diseases (3). In obese subjects, hypertrophied adipocytes display abnormal secretion of leptin and adiponectin and increased production of numerous inflammatory cytokines and chemokines, leading to a disrupted interorgan communication between VAT and important metabolic peripheral tissues such as liver and skeletal muscle (4). These organs are particularly exposed to free fatty acids and cytokines, mostly interleukin (IL)-6, which are increasingly released by the visceral fat of obese subjects (5,6). Skeletal muscles are one of the major metabolic tissues of the body, playing a pivotal role in glucose and lipid metabolism. There is a growing body of evidence showing the effects of obesity on skeletal muscle dysfunction, such as the development of insulin resistance, as attested to by numerous studies performed

[1]INSERM, U1166 Nutriomique, Paris, France
[2]Sorbonne Universités, University Pierre et Marie Curie-Paris 6, UMR S 1166, Paris, France
[3]Institut Cardiométabolisme et Nutrition, Pitié-Salpétrière Hospital, Paris, France
[4]Metabolic Research Laboratories, Wellcome Trust-MRC Institute of Metabolic Science, University of Cambridge, Cambridge, U.K.
[5]Sorbonne Universités, University Pierre et Marie Curie-Paris 6, Centre de Recherche en Myologie, UMR 974, Paris, France
[6]INSERM, U974, Paris, France
[7]CNRS FRE 3617, Paris, France
[8]Institut de Myologie, Paris, France

Corresponding author: Vanessa Pellegrinelli, vp332@medschl.cam.ac.uk.

Received 19 May 2014 and accepted 10 February 2015.

This article contains Supplementary Data online at http://diabetes.diabetesjournals.org/lookup/suppl/doi:10.2337/db14-0796/-/DC1.

K.C., G.S.B.-B., and D.L. share senior co-authorship.

See accompanying article, p. 3055.

in rodent models of obesity (7,8). Thus, it has been shown that obese rats display impaired activation of skeletal muscle protein synthesis in response to chronic lipid infiltration (9). Ectopic lipid storage in muscle (i.e., within muscle cells and/or in adipocytes located between muscle fibers) represents a negative risk factor for the development of type 2 diabetes related to muscle insulin resistance (10–13). Moreover, skeletal muscle of obese subjects also displays an impairment in oxidative capacity (14) and abnormal muscle fiber organization (15,16). An increased amount of VAT in obesity has been proposed to link obesity and muscle metabolic alterations, such as insulin resistance. Surgical removal of VAT in rats leads to a reduction of systemic concentrations of cytokines (e.g., IL-6, fractalkine resistin) and improvement of skeletal muscle insulin sensitivity (17). Particularly, adipocytes have been identified as potential effectors of muscle cell dysfunction. A coculture system previously showed the impact of adipocytes on muscle cell insulin resistance and oxidative capacity (18–20). However, the impact of VAT adipocytes on muscle structural organization and the molecular factors involved remains elusive. Inflammatory mediators act synergistically to negatively impact regeneration capacity and insulin sensitivity in muscle (7). For example, IL-6 is overproduced by hypertrophied adipocytes, and its systemic concentration is increased in obesity. Increased IL-6 is associated with altered insulin signaling in myotubes and with impaired myoblast differentiation/proliferation capacity, leading to muscle atrophy (7,8). At the molecular level, IL-6 with IL-1β downregulates IGF/Akt signaling, decreasing muscle protein synthesis (21). Excessive production of various mediators by obese VAT adipocytes could trigger a cross talk with muscle cells, altering the production of myokines (22), which could, in turn, affect VAT endocrine functions. This cross talk associated with an inflammatory microenvironment could be deleterious in perpetuating a vicious cycle leading to muscle loss and wasting. To address this question, the secretome of obese adipocytes was tested on human primary muscle cells, and direct cocultures were performed.

The main aim of our study was to identify the major contributors of VAT adipocytes/skeletal muscle cross talk and their role in inducing muscle atrophy and inflammation, which are common disorders that are associated with metabolic pathologies such as obesity and type 2 diabetes (4).

RESEARCH DESIGN AND METHODS

The antibodies and recombinant proteins used in the study are listed in Supplementary Table 1.

Mouse Studies

C57BL/6N male mice were purchased from Charles River Laboratories. Standard chow or the 58 kcal% fat with sucrose Surwit Diet (high-fat diet [HFD]; catalog #D12331; Research Diets) was given ad libitum to the animals. Dietary intervention started at 8 weeks of age and continued for 12 or 16 weeks (n = 8–9 per experimental group). The detailed procedures of the mouse studies are provided in the study by Whittle et al. (23). Adipose tissue and skeletal muscle from 12-week-old chow/HFD mice (RNA extraction) and gastrocnemius muscle of 16-week-old chow/HFD mice (histological analysis) were prepared as described in the studies by Whittle et al. (23) and Riehle et al. (24). Muscle fiber cross-section size (up to 201 muscle fibers/section) was automatically evaluated by the determination of the Feret's diameter (ImageJ software) in three independent fields in each section. The variance coefficient of the Feret's diameter was defined to evaluate the muscle fiber size variability between the experimental groups of mice and to avoid experimental errors such as the orientation of the sectioning angle (25). The number of intermuscular adipocyte spots was assessed visually in the total longitudinal section biopsy sample.

Human Studies

SAT and VAT biopsy samples were obtained from morbidly obese subjects (BMI >40 kg/m^2) (clinical parameters are shown in Supplementary Table 2), and SAT biopsy samples were obtained from lean female subjects (BMI <25 kg/m^2) who were undergoing elective surgery. None of the lean subjects had diabetes or metabolic disorders, and none were receiving medication. All clinical investigations were performed according to the Declaration of Helsinki and were approved by the Ethical Committee of Hôtel-Dieu Hospital (Paris, France).

Isolation of Mature Adipocytes From Human WAT and Preparation of the Three-Dimensional Adipocyte Cultures

Tridimensional gels were prepared with mature adipocytes isolated from WAT of lean (SAT) or obese (SAT and VAT) subjects, as described in studies by Pellegrinelli et al. (26,27). Adipocytes were embedded in the hydrogel (PuraMatrix; BD Biosciences, Bedford, MA). Hydrogel was diluted in a 20% sucrose solution at a concentration of 1×10^5 cells/1 mL gel preparation into 24-well plates containing 1.5 mL of DMEM/F12 (1% bovine albumin, 1% antibiotics). The culture medium was changed after 1 h with fresh medium containing human insulin (50 nmol/L). Adipocytes from SAT or VAT were incubated for 48 h before collecting the conditioned media (CM) referred as lean SAT adipocyte CM (SAT CM) and obese SAT/VAT adipocyte CM (SAT/VAT CM), respectively. Samples were kept at −80°C prior to experimental measurements.

Myoblast Cultures, Differentiation From Myotubes, and Treatment With Adipocyte CM

We used the human primary satellite cells (CHQ5B cells) that were originally isolated from the quadriceps of a newborn child who had no indication of neuromuscular disease, as previously described (28). The cells were cultivated in a growth medium consisting of 4 vol DMEM, 1 vol M199 supplemented with 50 μg/mL gentamycin,

and 20% FBS. Cells were plated in 24-well plates at a density of 1,500 cells/cm^2. Differentiation was induced at subconfluence by replacing the growth medium with differentiation medium (DMEM supplemented with 50 μg/mL gentamycin and 10 μg/mL human insulin) (29). After 5 days of differentiation, the medium was replaced for 48 h with control DMEM/F12 culture medium or CM from either lean SAT CM or obese SAT/VAT CM. Then the medium was exchanged for fresh medium for 24 h before being collected and stored at −80 C.

Quantification of the Fusion Index and Measurement of Myotube Thickness

Muscle cells were allowed to differentiate in serum-free medium for 6 days in the presence of lean SAT CM or obese SAT/VAT CM. After fixation with 4% paraformaldehyde, the cells were incubated with an antibody specific for desmin. Specific antibody binding was revealed using an Alexa Fluor 488–coupled goat anti-mouse secondary antibody. Nuclei were visualized with Hoechst staining.

The efficiency of the fusion was assessed by counting the number of nuclei in myotubes (more than two myonuclei) as a percentage of the total number of nuclei (mononucleated and plurinucleated). This percentage was determined by counting 1,000 nuclei per dish on three independent cultures.

Myotubes thickness was quantified with ImageJ software measuring intensity of the desmin staining in 10 random fields (×10) from three independent cultures.

The counting was performed by two different investigators (V.A. and F.E.-V.) that were blind to experimental conditions.

Direct Cocultures of Primary Adipocytes and Differentiated Myoblasts in Three-Dimensional Hydrogels

Muscle cells were embedded in hydrogel, which was prepared as described below, at a concentration of 200,000 cells/100 μL gel preparation containing 0.5 mg/mL collagen type 1 (BD Biosciences). The gel preparation was put into 96-well plates containing 150 μL growth medium. After 2 days in culture, this medium was replaced by a differentiating medium for 3 days. We then added to this preparation a second hydrogel containing mature adipocytes isolated from VAT or SAT from obese subjects (10,000 cells/100 μL gel preparation). Adipocytes and differentiated myoblasts were then cocultured for 24 h or 3 days in DMEM/F12 (1% antibiotics and 50 nmol/L insulin).

Secretory Function Analysis and Serum Biochemistry

Adipokine secretions were evaluated by ELISA, using secretory medium from 24-h cultures of three-dimensional (3D) adipocytes (leptin, adiponectin) (DuoSet; R&D Systems). Concentrations of human cytokines were determined in CM from adipocytes, myotubes, or cocultures using human cytokine/chemokine Panel I 41plex from Millipore (Billerica, MA), as previously described (30). IGF-II levels were measured by ELISA in CM from myotubes cocultured or not with 3D adipocytes during 48 h of incubation. Serum levels of the murine cytokines IL-6, IL-1β, IL-10, and tumor necrosis factor-α were analyzed using the MSD 7-Plex mouse proinflammatory cytokine high-sensitivity kit (product code K15012C-2; Meso Scale Discovery, Gaithersburg, MD) on the Meso Scale Discovery SECTOR Imager 6000. Results were calculated using the MSD DISCOVERY WORKBENCH software package. The lower limits of detection were as follows: C-X-C motif ligand (CXCL) 1/2/3 (3.3 pg/mL), IL-10 (5.0 pg/mL), IL-1β (2.3 pg/mL), IL-6 (16.8 pg/mL), and tumor necrosis factor-α (0.9 pg/mL).

Neutralizing Experiments and Treatment by Recombinant Proteins

Myotubes alone or cocultured cells were treated with IgG1 (3 μg/mL) (MYO IgG, and MYO+AD IgG) or with IL-6 (2.5 μg/mL) and IL-1β (0.5 μg/mL) neutralizing antibodies (MYO abIL-6/IL-1β, MYO+AD abIL-6/IL-1β) over 3 days with renewal every day. Human recombinant IL-6 (10 ng/mL) and IL-1β (1 ng/mL) were added to myotubes cultured in the hydrogel for 3 days with renewal every day. In another set of experiments, myotubes and cocultured cells were treated with IGF-II (50 ng/mL) and insulin growth factor binding protein-5 (IGFBP-5) (200 ng/mL), when indicated, for 3 days with change every day. After this period, cells and media were collected for immunofluorescence and multiplex analysis, respectively.

Immunofluorescence Analysis and Confocal Microscopy

After fixation in 4% paraformaldehyde, cells were processed for immunofluorescence analysis. These samples were incubated with the appropriate primary antibody (overnight at 4°C), and then with the corresponding Alexa Fluor 488–conjugated anti-mouse IgG or Alexa Fluor 546–conjugated anti-rabbit IgG interspaced by multiple washes in PBS, and followed by mounting on coverslips. Sample examinations were performed at the imaging platform (Centre d'Imagerie Cellulaire et de Cytométrie [CICC], Centre de Recherche des Cordeliers, Paris, France) using a Zeiss 710 confocal laser-scanning microscope (Carl Zeiss, Inc., Thornwood, NY) fitted with an LD LCI Plan-Apochromat oil-immersion objective ×25 or ×63. Images were captured and analyzed with ZEN 2009 imaging software (Carl Zeiss, Inc.).

Western Blot Analysis

Total cell extracts were prepared in a buffer containing a cocktail of protease and phosphatase inhibitors (Roche Diagnostics, Mannheim, Germany) and were analyzed as previously described (26). Apparent molecular sizes were estimated by using the SeeBlue Plus2 Pre-Stained Protein Standard (Life Technologies, Foster City, CA), as indicated on immunoblots.

RNA Preparation and PCR Array

Muscle cells and adipocytes cocultured in the 3D scaffolds were processed for RNA extraction using the RNeasy RNA Mini Kit (Qiagen, Courtaboeuf, France). After reverse transcription of the total RNAs (1 μg), samples were analyzed by *1*) real-time PCR and *2*) PCR array using the "human myogenesis and myopathy PCR array" according to

the manufacturer's instructions (Qiagen). Supplementary Table 3 presents the list of the primers used. Data were normalized according to the RPLPO gene expression. The list in the Supplementary Data presents the functional classification of the genes in the human myogenesis and myopathy PCR array.

Statistical Analysis

The experiments were performed at least three times, using adipocytes from different human subjects. Statistical analyses were performed with GraphPad Software (San Diego, CA). Values are expressed as the mean ± SEM of (n) independent experiments performed with different adipocyte preparations. Comparisons between the two conditions in the in vitro experiments (adipocytes and adipocytes/myotubes cultures) and in vivo studies (chow and HFD mice) were analyzed using the Wilcoxon nonparametric paired test. Comparisons between more than two groups were performed using one-way ANOVA followed by post hoc tests. Spearman coefficients were calculated to examine the correlations. Differences were considered significant when $P < 0.05$.

RESULTS

Adipocyte Secretions From Obese VAT Provoke Muscle Cell Dysfunctions

Obesity and associated metabolic disorders such as type 2 diabetes are associated with muscle dysfunction characterized by inflammation and fat deposition (7). The muscle alterations are associated with insulin resistance linked with an increase of visceral fat mass (10,20,31). We sought to establish whether SAT/VAT from obese subjects could directly contribute to the harmful phenotype observed in the muscle of these patients. Here, we take advantage of a well-characterized cohort of severely obese subjects showing chronic inflammation and marked insulin resistance (1,32), as shown in Supplementary Table 2.

Initially, we characterized the secretomes of obese SAT CM and obese VAT CM obtained from obese subjects and the media obtained from the adipocytes isolated from the SAT of healthy lean subjects as controls (lean SAT CM). As expected, low adiponectin secretion was observed in obese SAT and VAT adipocytes compared with lean SAT adipocytes (Supplementary Fig. 1*A*). We observed that the secretome of VAT adipocytes exhibited a proinflammatory profile with high levels of several cytokines (IL-6 and granulocyte colony-stimulating factor [G-CSF]), chemokines (IL-8, C-C motif ligand [CCL] 2, CCL5, and CXCL1/2/3), as well as fibroblast growth factor-2, compared with SAT adipocytes from either lean or obese subjects (Supplementary Fig. 1*A* and *B*). Adipocytes from obese SAT presented an intermediary inflammatory profile between lean SAT and obese VAT.

For this reason, we focused on obese VAT adipocytes and explored the impact of VAT CM on myotube morphology and contractile protein expression, in comparison with lean SAT CM. We observed that myotubes were thinner in the presence of obese VAT CM than under control and lean SAT CM conditions, as estimated after immunofluorescence staining with desmin (a major component of muscle cell architecture and contractility), which was also significantly lower in myotubes treated with obese VAT CM than with lean SAT CM (−20%, $P < 0.01$) (Fig. 1*A* and *B*). The number of nuclei in the differentiated cultures was not modified by the two CM (Fig. 1*C*). Western blot analysis showed that myosin heavy chain (MF20) and troponin, two major components of the contractile apparatus in skeletal muscle, were also significantly decreased for both proteins in the presence of obese VAT CM compared with control and lean SAT CM conditions (Fig. 1*D*). If lean SAT seems to impact myotube thickness and protein content, this was not statistically significant and remained at a much lower level than the effect of obese VAT CM. These data suggest that the secretome of obese VAT adipocyte decreases the myogenic capacity of the skeletal myoblasts.

VAT Adipocytes Directly Induce Muscle Cell Atrophy in a 3D Scaffold

We then examined the effect of obese SAT and VAT adipocytes on skeletal muscle cells by using 3D cocultures. Mature adipocytes and muscle cells were then embedded in separate hydrogels (Supplementary Fig. 2*A* and *B*), which were previously characterized by the ability to maintain altered functions of obese adipocytes (26). Direct cocultures of human cells in a 3D setting are of great value because they allow the study of a complex set from adipocyte-derived signals that regulate skeletal muscle functions without confounding the effects of other organ systems, while maintaining signals including labile diffusible factors. The human myoblast differentiation and fusion processes were not modified by cultivation in this 3D scaffold compared with two-dimensional cultures (see MF20 and DAPI staining) (Supplementary Fig. 2*C*).

We used a skeletal muscle–specific PCR array to determine the effects of the obese VAT adipocytes on the expression of the muscle-specific genes. Among the set of 86 genes screened on the array, we detected significant underexpression of 10 genes in the muscle cells exposed to obese VAT adipocytes. Especially, we found decreased levels of myogenic transcription factors MyoD1 and myogenin (MYOG); the growth factor IGF-II and its binding partner IGFBP-5; the sarcomeric protein titin, a member of the dystrophin complex; α-sarcoglycan; the muscle-specific protein of caveolae, caveolin-3; and an important component of the neuromuscular junction, the muscle-specific kinase (Fig. 2*A*). It should be noted that endoplasmic reticulum (ER) stress and cytolysis pathways were not detected in the cocultured cells, as assessed from the expression of ER stress markers (ATF4, HSPA5, and C/EBPζ) and lactate dehydrogenase activity, respectively (Supplementary Figs. 3 and 4*A*).

By confocal analysis, we confirmed the decreased expression of titin at the protein level in myotubes induced by VAT adipocytes (Fig. 2*B*). Moreover, myotubes

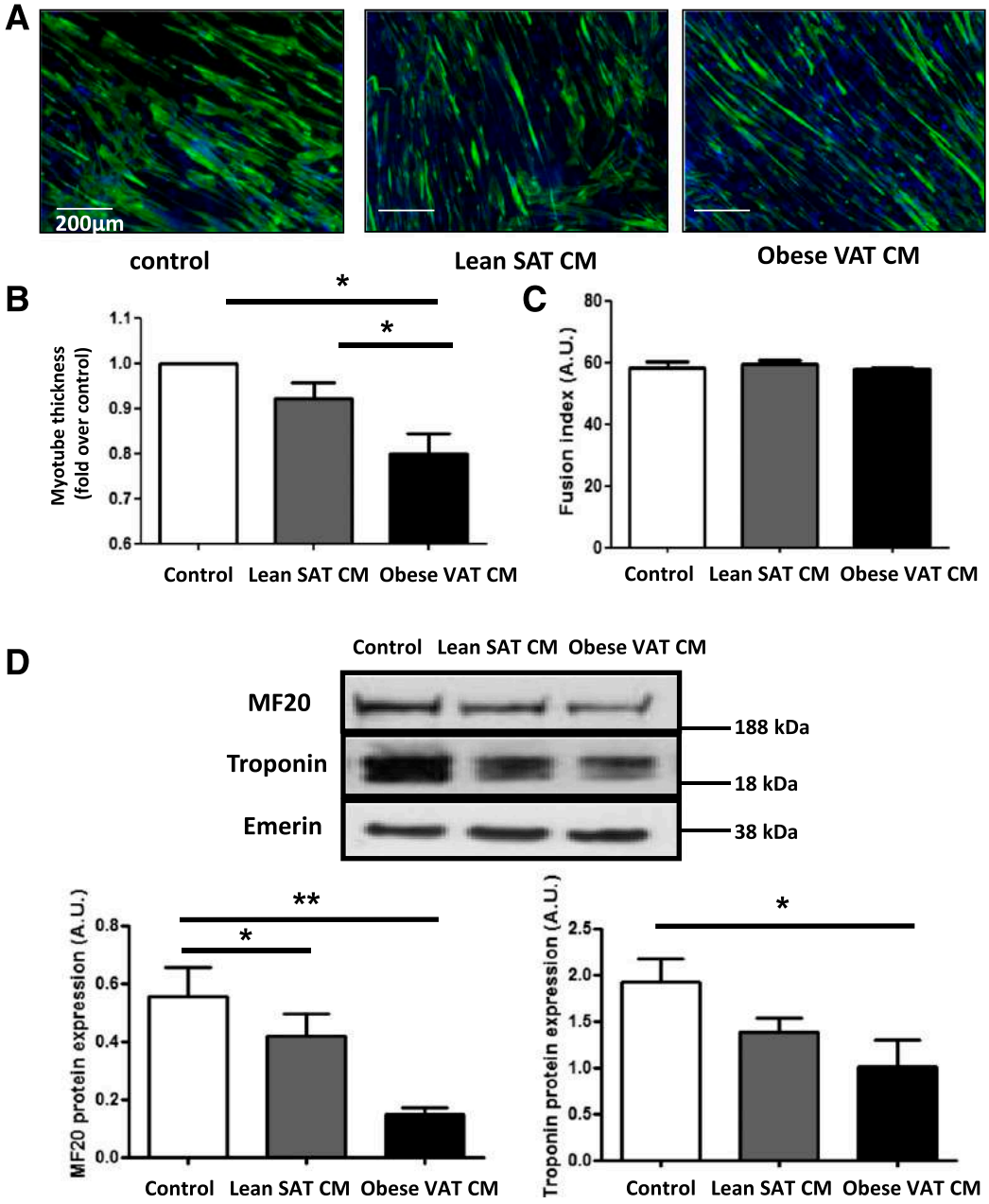

Figure 1—Human adipocyte secretions and myotube phenotype. *A*: Human differentiated muscle cells were cultured in the presence of lean SAT CM or obese VAT CM for 5 days. Cells were incubated with an antibody specific for desmin, which was revealed using an Alexa Fluor 488–coupled goat anti-mouse secondary antibody (green). Nuclei were visualized with Hoechst staining (blue). A representative photomicrograph is presented. Scale bar = 200 µm. *B*: Myotube thickness was quantified using ImageJ software measuring intensity of the desmin staining in 10 random fields (×20) in three independent cultures. *C*: Fusion index: the number of nuclei in differentiated myotubes (more than two myonuclei) were calculated as a percentage of the total number of nuclei (mononucleated and plurinucleated). A total of 1,000 nuclei/dish was counted in three independent cultures. The counting was performed with blind lectures by different investigators (V.A. and F.E.-V.). *D*: Cell lysates were immunoblotted to detect the heavy chain of myosin II (MF20; 200 kDa), troponin (24 kDa), and emerin (37 kDa; used as normalization control). Graphs represent the quantification of the immunoblots. Data are the mean ± SEM of five independent experiments. $^{*}P < 0.05$, $^{**}P < 0.01$, control vs. lean SAT CM or obese VAT CM. A.U., arbitrary units.

exposed to VAT adipocytes showed a reduced striated staining for titin, suggesting a disturbed internal sarcomeric structure (Fig. 2*C*).

Importantly, when compared with obese VAT adipocytes, obese SAT adipocytes appeared less potent in inducing muscle cell atrophy, as seen from myotube thickness and the staining of troponin and titin (Fig. 2*D–F*).

Next, we quantified the levels of inflammation-related proteins using a multiplex "human cytokines/chemokines"

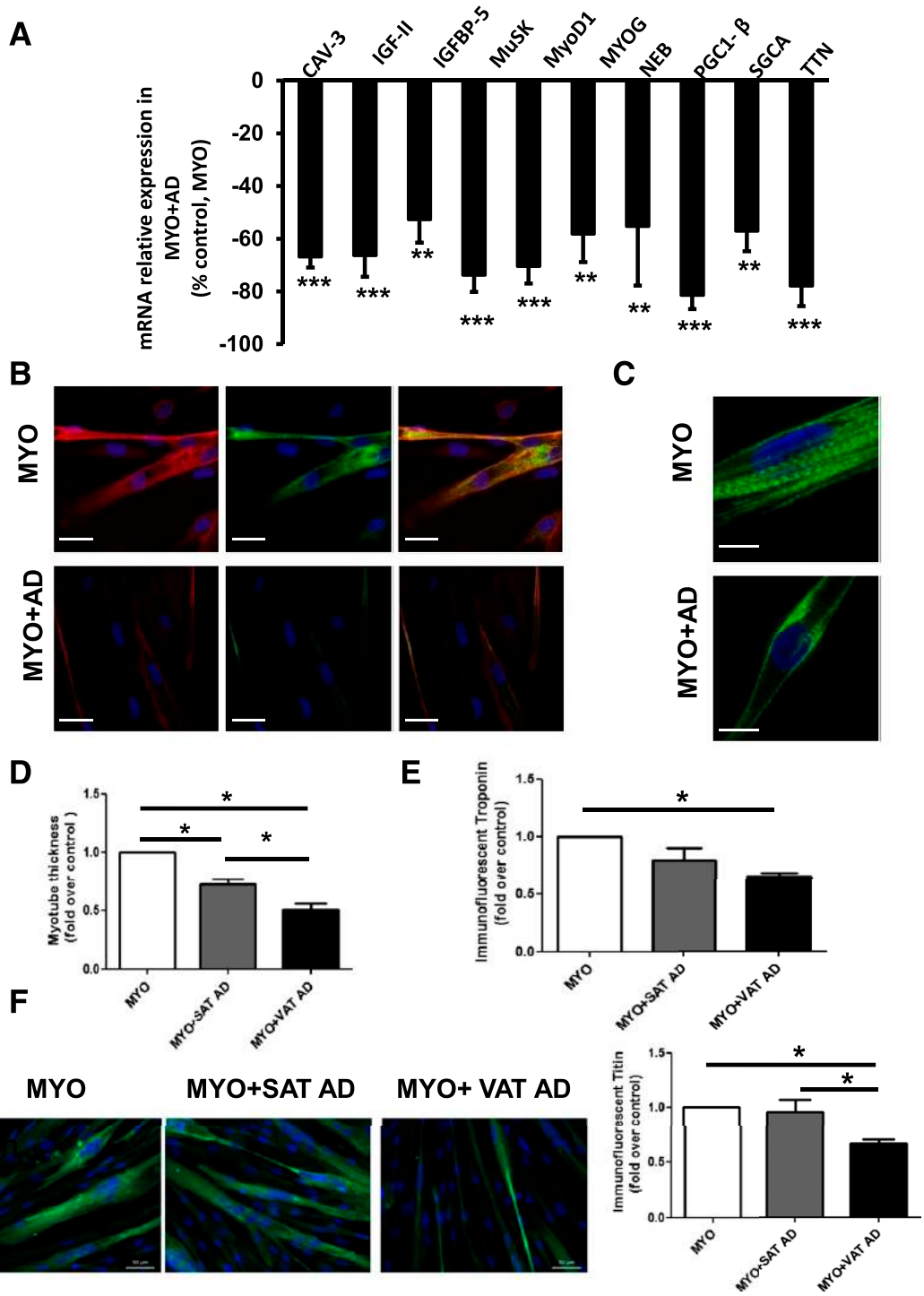

Figure 2—Gene expression profile of myocytes cocultured with human adipocytes. Muscle cells were differentiated in the 3D hydrogel for 3 days, and then VAT adipocytes in the 3D hydrogel were added for an additional period of 1 day. Cells were then collected for RNA extraction obtained after reverse transcription cDNAs. *A*: cDNAs were analyzed using a human myogenesis and myopathy PCR array. The graph represents the percentage of decreased gene expression in myocytes cocultured with adipocytes (MYO+AD) compared with myocytes alone (control, MYO). Data are presented as the mean ± SEM of five independent experiments. $^{**}P < 0.01$, $^{***}P < 0.001$, MYO+AD vs. MYO. *B* and *C*: Cells were also fixed and stained using antibody directed against titin (green, Alexa Fluor 488–conjugated anti-mouse IgG) and phalloidin (red, Alexa Fluor 546 phalloidin). A representative photomicrograph from confocal microscopy is presented. Scale bars: *C*, 20 μm; *D*, 10 μm. *D–F*: Muscle cells were differentiated for 3 days, and then 3D adipocytes from SAT or VAT from paired biopsy samples of obese subjects were added for an additional period of 3 days. Cells were fixed and stained using antibody directed against desmin, troponin, or titin (green, Alexa Fluor 488–conjugated anti-mouse IgG). Graphs represent quantifications of myotube thickness (*D*), troponin staining (*E*), and titin staining (*F*). Data are the mean ± SEM of six to eight independent experiments. $^{*}P < 0.05$, MYO+VAT AD vs. MYO. CAV-3, caveolin-3; MuSK, muscle-specific kinase; NEB, nebulin; SGCA, α-sarcoglycan; TTN, titin.

approach. Among the 41 screened proteins, 12 were significantly detected in VAT adipocytes and myocytes (level >15 pg/mL). CCL2, IL-8, CXCLs, G-CSF, IL-6, and vascular endothelial growth factor were highly secreted by the cocultured cells compared with VAT adipocytes grown alone in hydrogel (Supplementary Fig. 4*B*). For most of these inflammatory proteins, secretion was increased in an additive manner in the presence of myotubes and adipocytes. Moreover, a synergistic effect was observed for G-CSF (75-fold, $P < 0.05$), IL-6 (25-fold, $P < 0.05$), and CCL7 (10-fold, $P < 0.01$) (Fig. 3*A*). As observed above for muscle cell atrophy, adipocytes from obese SAT provoked a lower inflammatory status than those from obese VAT in the cocultured cells (Fig. 3*B* and *C*). Considering the marked inflammatory profile of VAT adipocytes from obese subjects and their potent impact on muscle cell phenotype compared with lean and obese SAT adipocytes, we then focused on the cross talk between muscle cells and obese VAT adipocytes.

IL-6 and IL-1β Have a Relevant Role in Inflammation of Myotubes/Adipocytes

We tested the role of the two proinflammatory cytokines IL-6 and IL-1β as drivers of myotube inflammation observed in cocultures based on previous reports (26,33,34). After 3 days of culture, in the presence of the neutralizing IL-6/IL-1β antibodies, the inflammatory response of cocultured cells was reduced with decreased levels of G-CSF (−71.4%); fractalkine (−58%); IL-7 (−56%); and the chemokines CXCL1/2/3 (−53%), CCL7 (−42%), IL-8 (−43.5%), interferon-γ–induced protein-10 (−36%), and CCL5 (−38%) (Fig. 3*D*). To further confirm the role of IL-6/IL-1β, we treated myotubes with human recombinant IL-6 and IL-1β, which showed marked increased secretion of inflammatory molecules such as G-CSF (~6,000-fold), CXCL1/2/3 (~100-fold), and IL-8 (~100-fold) ($P < 0.001$) (Fig. 3*E*). These results indicate the key role played by the cytokines IL-6 and IL-1β in the inflammatory environment of the cocultured cells. Strikingly, the combination of recombinant IL-6/IL-1β or antibody neutralization of endogenous IL-6/IL-1β failed to influence myotube thickness and titin staining (Supplementary Fig. 5), suggesting an independent relationship between inflammation and the atrophic phenotype observed in our experimental conditions.

IGF-II and IGFBP-5 Correct the Myotube Atrophy Induced by Obese VAT Adipocytes

As shown in Fig. 2*A*, myotubes cocultured with obese VAT adipocytes displayed a decreased expression of IGF-II and its binding partner IGFBP-5, which are known to synergically promote myogenic action (35). In 3D cultures of myocytes, 3 days of treatment with human recombinant IGF-II (50 ng/mL) and IGFBP-5 (200 ng/mL) impacts muscle cells by increasing titin content (Supplementary Fig. 6). We then tested the potential correction of the atrophic phenotype of myotubes cocultured with VAT adipocytes. Interestingly, long-term treatment with IGF-II and IGFBP-5 corrected the atrophic aspect of the cocultured myotubes through increased thickness (Fig. 4*A*) and the production of both titin and myosin heavy chain (Fig. 4*B–D*).

However, long-term treatment with IGF-II/IGFBP-5 failed to decrease the inflammatory secretome of the cocultured cells (Supplementary Fig. 7). Conversely, cocultured cells treated by neutralizing antibodies for IL-6 and IL-1β or treatment of myotubes by recombinant IL-6 and IL-1β did not influence the production of IGF-II (Supplementary Fig. 5*A*).

Downregulation of the Signaling Pathways Controlling Protein Synthesis in Myotubes Exposed to VAT Adipocytes

Skeletal muscle mass is determined by the balance between protein synthesis and degradation. The rate of protein synthesis is, at least in part, finely controlled by the phosphoinositide 3-kinase/Akt/mammalian target of rapamycin signaling pathway, which is activated by IGFs and amino acids (36). Here, we assessed the IGF-II/IGFBP-5 activation of this pathway in cocultured atrophic myotubes by measuring the phosphorylation status of direct targets Akt, p70S6K, and 4E-BP1. We showed a reduction of basal phosphorylation of Akt, S6K, and 4E-BP1 in cocultured myotubes compared with control myotubes as well as reduced AKT phosphorylation in response to IGF-II/IGFBP-5 (Fig. 4*E* and *F*), suggesting that signaling pathways (Akt/S6K/4E-BP1) controlling protein synthesis are downregulated in cocultured muscle cells. Conversely, the gene expression of two atrophy-related ubiquitin ligases, atrogin-1 and murf-1, remained unchanged in muscle cells exposed to VAT adipocytes and were not influenced by IGF-II/IGFBP-5 (Supplementary Fig. 8). Overall, our data suggest that the atrophy phenotype is likely related to decreased synthesis of muscle proteins.

Diet-induced obesity induces muscle atrophy in association with epididymal WAT hypertrophy and the accumulation of intermuscular adipocytes in mouse models.

In order to validate in vivo the relevance of the molecular candidates identified from our 3D cocultures, we used a diet-induced obese mouse model and screened the expression of inflammatory/muscle markers in their skeletal muscles. After 12 weeks of eating an HFD, mice displayed WAT and systemic inflammation with a global decrease in the gene expression of muscular markers such as MyoD (−76%), IGF-II (−58%), β-actin (−43%), and peroxisome proliferator–activated receptor γ coactivator (PGC)-1β (−30%) in the gastrocnemius muscle (Fig. 5*A* and *B* and Supplementary Fig. 9*A*). Conversely, the expression of the inflammatory markers IL-1β and CCL2 was significantly increased (1.7-fold [$P = 0.0415$] and 1.5-fold [$P = 0.0361$], respectively). In addition, the expression of skeletal muscle markers such as MyoD and IGF-II was negatively correlated with increased fat mass (percentage of fat mass and leptin expression) and

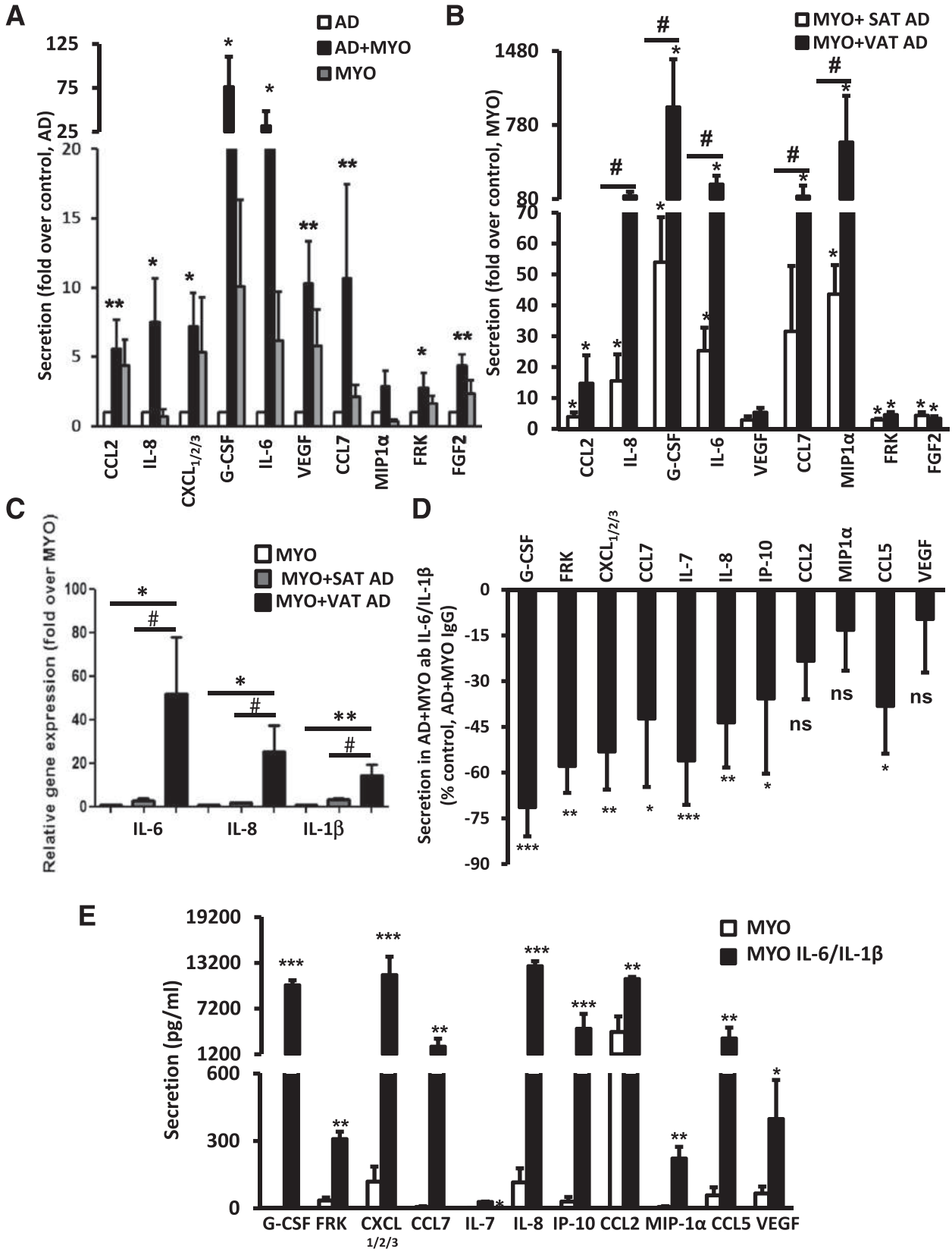

Figure 3—Inflammatory profile of cocultured human adipocytes and myocytes: IL-6 and IL-1β as key factors. Muscle cells were differentiated in the 3D hydrogel for 3 days, and then SAT or VAT adipocytes from obese subjects, cultured in the 3D hydrogel, were added for an additional period of 3 days. Media were then collected for the measurement of cytokine and chemokine secretion by a multiplex assay. *A*: Significant changes in the secretory profile in the 3D cultures of muscle cells and obese VAT adipocytes (AD+MYO) compared with AD as control and MYO are presented in the graph. Data are expressed as fold variations between AD (white bars), AD+MYO (black bars) and

inflammation in epididymal WAT (IL-6 expression) (Table 1 and Supplementary Table 4). However, we did not find any correlations between IL-6 expression in inguinal WAT and skeletal muscle markers, highlighting the specificity of the cross talk between muscle and the VAT depots (Supplementary Table 5). Finally, histological analysis of the gastrocnemius muscle of obese mice revealed pathological changes generally observed in the muscle of dystrophic mice (25) with abnormal distribution of the muscle fiber size in cross-sectional samples (increased covariance coefficient of Feret's diameter) and adipocyte accumulation (Fig. 5*C–E* and Supplementary Fig. 9*B*). Accordingly, we observed an increased expression of adipocyte markers (i.e., leptin and fatty acid binding protein-4) in muscle of obese mice, reflecting increased fat infiltration (Supplementary Fig. 9*C*). Interestingly, the expression of MyoD, IGF-II, and β-actin in skeletal muscle was negatively correlated with leptin expression in epididymal WAT and skeletal muscle (Table 1). These results suggest a potential relationship between adipocyte accumulations and muscle structure and dysfunction.

DISCUSSION

We studied the adipocyte/muscle cell cross talk participating in the complex intertissular network of hypertrophied WAT with skeletal muscle. Here, using a 3D coculture system, we provide evidence in vitro that adipocytes from obese VAT induce muscle cell inflammation and atrophy by decreasing the expression of contractile proteins such as troponin, titin, and myosin heavy chain. Importantly, we showed that in obese states, VAT adipocytes are more potent than their SAT counterparts in provoking deleterious effects in muscle cells, such as atrophy and inflammation. These observations are probably linked to differences in the lineage specificity and tissular environment characterizing these two depots (1,2,37,38).

Coculture systems have been developed during the last decade to study the cross talk between adipose tissue and muscle, particularly focusing on the impact of adipocytes on muscle insulin resistance and glucose uptake. Cocultures of human in vitro differentiated preadipocytes with skeletal muscle cells induce the insulin resistance of the latter (19) by an impact on oxidative metabolism (20). Here we have used mature (i.e., unilocular) adipocytes isolated from human subjects. These cells display high metabolic (lipolytic activity) and secretory (production of leptin and adiponectin) functions compared with in vitro differentiated preadipocytes. We believe that the results obtained using this 3D setting with mature adipocytes may be more pathophysiologically relevant than previous studies using a two-dimensional coculture with primary human myoblasts (18–20,39). In addition, this system allowed a long-term survey of muscle cell functions addressing the original question of the impact of obese VAT adipocytes on inflammation and myotube structural organization.

Our results reveal that cocultures of obese VAT adipocytes with muscle cells enhanced the proinflammatory environment with increased production of several cytokines (IL-6 and G-CSF) and chemokines (CCL2, IL-8, CXCL1/2/3, CCL7, and fractalkine). More importantly, we have clearly identified IL-6 and IL-1β as playing key roles in this inflammatory loop. These cytokines, which act in concert in various inflammatory processes, are overproduced by adipose tissue during obesity and type 2 diabetes (40,41).

Muscle cells are characterized by their contractile capacity, a phenomenon depending on tissue physical properties. The hydrogel used in the current study is soft (~300 Pa, compared with skeletal muscle or culture well plates, ~12 and ~100 kPa, respectively) (42), limiting the analysis of myotube contractility in our 3D cocultures. However, in this 3D model maintaining adipocyte viability, we were able to demonstrate a major role of obese VAT adipocytes on inducing muscle cell atrophy phenotype. The myogenic program is controlled by transcription factors such as MyoD and MYOG. The binding of these factors to specific sequences in the promoter of muscle-specific genes increases the expression of contractile proteins such as myosin

MYO (gray bars) to take into account human interindividual variations. Data are presented as the mean ± SEM of seven independent experiments. **P* < 0.05, ***P* < 0.01 AD+MYO vs. AD. *B*: Significant changes in the secretory profile in the 3D cultures of muscle cells and obese SAT (MYO+SAT AD) or obese VAT adipocytes (MYO+VAT AD) are presented in the graph. Data are expressed as fold variations between MYO (control) and MYO+SAT AD (white bars) or MYO+VAT AD (black bars). Data are presented as the mean ± SEM of eight independent experiments. *C*: Gene expression of IL-6, IL-8, and IL-1β in muscle cells cultured alone (control, MYO, white bars) or exposed to adipocytes from paired biopsy samples of obese SAT (MYO+SAT AD, gray bars) or VAT adipocytes (MYO+VAT AD, black bars), estimated by real-time PCR. Data (fold over control, MYO) are presented as the mean ± SEM of six independent experiments performed with different adipocyte preparations. **P* < 0.05, ***P* < 0.01 MYO+VAT AD vs. MYO. #*P* < 0.05, MYO+SAT AD vs. MYO+VAT AD. *D*: 3D VAT adipocytes were added for an additional period of 3 days and were treated with neutralizing antibodies of IL-6 (2.5 μg/mL) and IL-1β (0.5 μg/mL) (MYO+AD+abIL-6/IL-1β) IgG1 (control MYO+AD IgG) in the 3D setting. Media were then collected for multiplex assay. Black bars represent the percentage decrease in secretions in MYO+AD+abIL-6/IL-1β cocultures compared with control MYO+AD IgG cocultures. Data are presented as the mean ± SEM of five independent experiments. **P* < 0.05, ***P* < 0.01, ****P* < 0.001, MYO+AD IgG vs. MYO+AD+abIL-6/IL-1β. *E*: Multiplex assay of the inflammatory secretome of myocytes treated (MYO IL-6/IL-1β, black bars) or not (MYO, white bars) with recombinant IL-6 (10 ng/mL) and IL-1β (1 ng/mL) over 3 days. Data are presented as the mean ± SEM of five independent experiments. **P* < 0.05, ***P* < 0.01, ****P* < 0.001 MYO IL-6/IL-1β vs. MYO. ab, antibodies; FRK, fractalkine; IP-10, interferon-γ–induced protein-10; MIP1α, macrophage inflammatory protein 1α; ns, nonsignificant; VEGF, vascular endothelial growth factor.

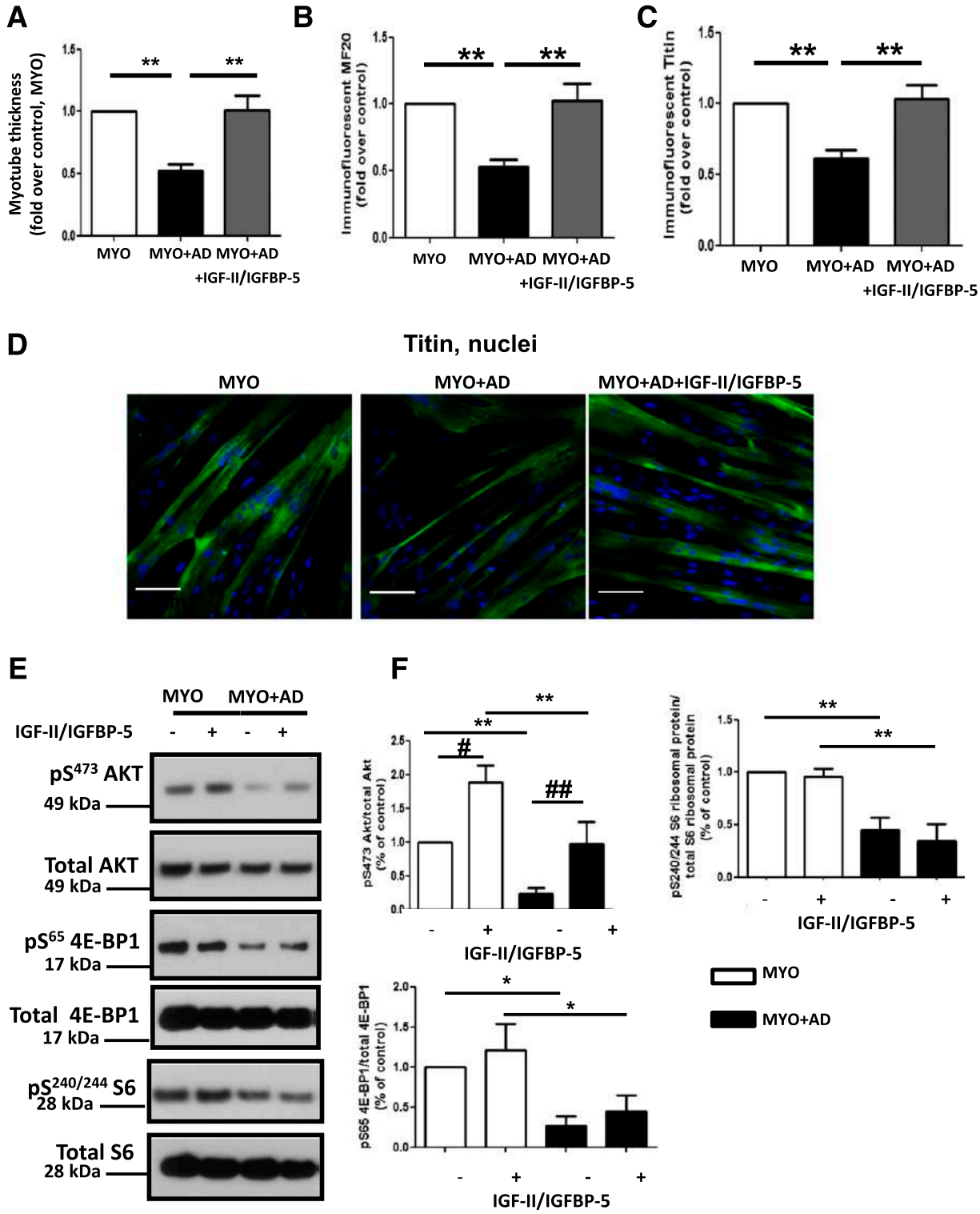

Figure 4—IGF-II and IGFBP-5 rescue the atrophy of myotubes induced by adipocytes. *A–D*: Muscle cells were differentiated in the 3D hydrogel for 3 days without (MYO) or with 3D VAT adipocytes (from obese subjects) (MYO+AD) added for an additional period of 3 days in the presence or absence of IGF-II (50 ng/mL) and IGFBP-5 (200 ng/mL) (MYO+AD+IGF-II/IGFBP-5). Cells were fixed and stained with the corresponding antibodies. *A*: Myotube thickness was quantified using ImageJ software measuring the intensity of the desmin staining in 10 random fields (×20) in six independent cultures. Quantification of immunofluorescence was performed using ImageJ software measuring intensity of the MF20 (*B*) and titin (*C*) staining in five random fields (×20). *D*: Immunostaining of titin (green, Alexa Fluor 488–conjugated anti-mouse IgG) and nuclei (blue, DAPI). A representative photomicrograph of titin staining is presented (scale bar = 50 μm). Data are presented as the mean ± SEM of six independent experiments. $^{**}P < 0.01$, MYO+AD vs. MYO or MYO+AD+IGF-II/IGFBP-5. *E* and *F*: Differentiated muscle cells exposed or not to obese VAT adipocytes were stimulated with IGF-II (50 ng/mL) and IGFBP-5 (200 ng/mL) for 10 min at 37°C. Serine 473 phosphorylation of Akt (pS 473 Akt, 56 kDa), serine 65 of 4E-BP1 (pS65 4E-BP1, 21 kDa), and serine 240 and 244 phosphorylation of S6 ribosomal protein (pS 240/244 S6 ribosomal protein, 32 kDa) were detected using the corresponding antibodies.

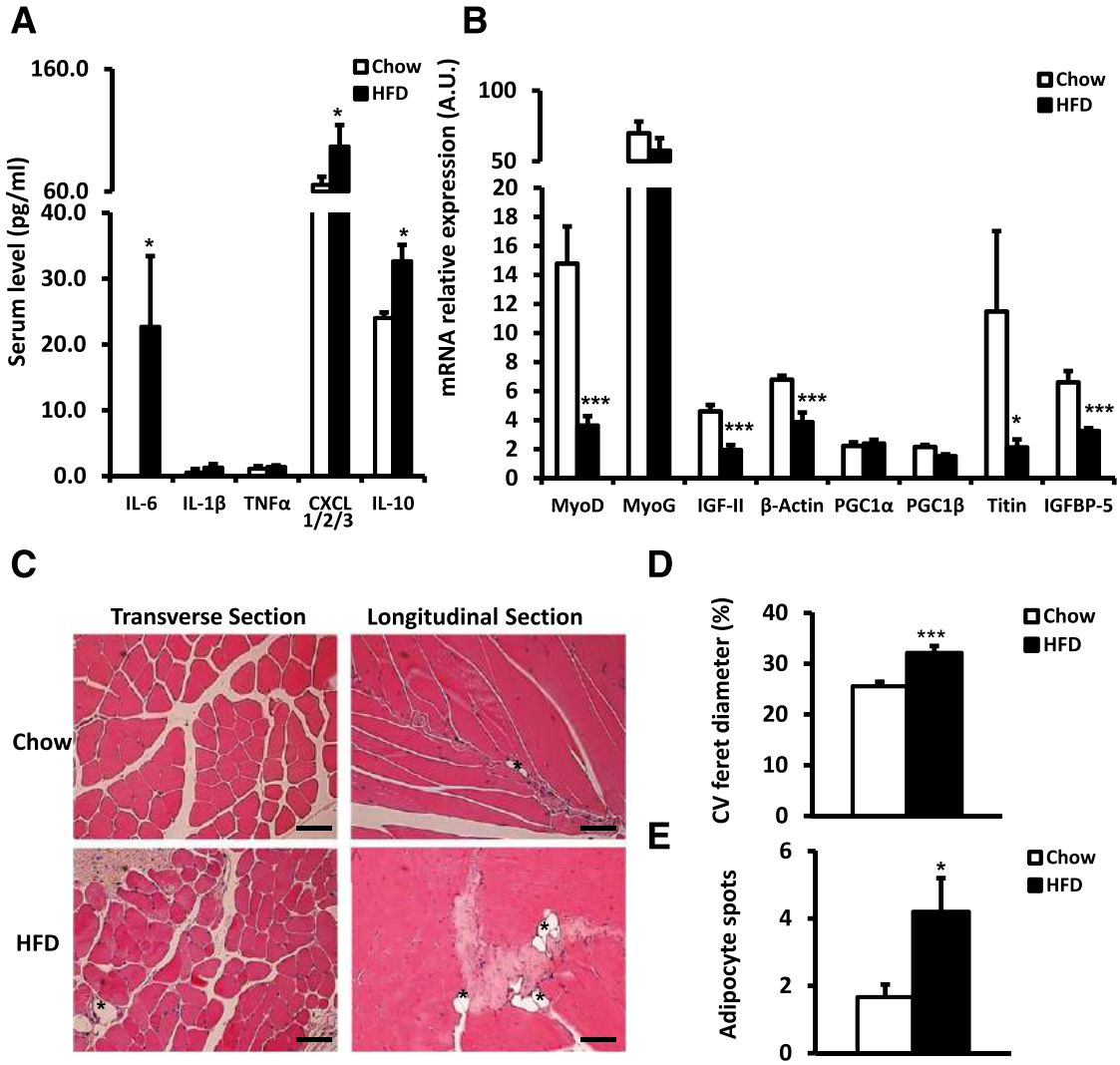

Figure 5—Skeletal muscle characteristics of HFD-induced obese mice. Serum cytokine level (*A*) and gastrocnemius gene expression (*B*) evaluated in 20-week-old mice after 12 weeks of being fed a standard diet (chow, white bars) or an HFD (black bars). n = 8 mice per experimental group. *C–E*: Histological analysis of the gastrocnemius muscle obtained from 24-week-old mice (n = 9 mice per experimental group) after 16 weeks of being fed a standard diet (chow) or an HFD. *C*: Representative microphotographs of a cross-section (right panel) and a longitudinal section (left panel). Scale bar = 100 μm. *D*: Measurement of variance coefficients of the fiber size in the cross-sectional samples of chow-fed and HFD-fed mice using Feret's diameter as the geometrical parameter. n = 61 (minimum) to 201 (maximum) fibers were analyzed for each sample (three random fields/mouse, ×10). *E*: Quantification of adipocyte spots in the longitudinal section samples of chow-fed and HFD-fed mice (total biopsy sample). *P < 0.05, ***P < 0.001, chow-fed vs. HFD-fed mice. A.U., arbitrary units; CV, coefficient of variation; ns, nonsignificant.

heavy chain, tropomyosin, troponin (43,44), and titin, which maintains sarcomere integrity (45). At the molecular level, we observed the downregulation of MyoD, MYOG, and contractile/sarcomeric proteins (titin) and the dystrophin complex in myotubes cocultured with the obese VAT adipocytes. These data provide new insights about which proteins are preferentially targeted and participate in the atrophic phenotype of the muscle cells when cocultured in this 3D setting.

In addition to the decreased gene expression of muscle-specific structural proteins, we also observed a decreased expression of the growth/myogenic factor IGF-II and its binding partner IGFBP-5 (35). IGF-II shares with IGF-I the same receptor and protein signaling pathway

E: A representative Western blot is presented among the five different experiments. *F*: The graph represents quantifications of the immunoblots in IGF-II/IGFBP-5–stimulated conditions normalized to total proteins. Data are presented as the mean ± SEM of five to seven independent experiments. *P < 0.05, **P < 0.01, MYO+AD vs. MYO. #P < 0.05, ##P < 0.01, without vs. with IGF-II/IGFBP-5 treatment.

Table 1—Spearman correlations between the gene expression of muscle markers in the skeletal muscle (gastrocnemius) and the expression of leptin/IL-6 in both epididymal adipose tissue and skeletal muscle

			Epididymal adipose tissue				Gastrocnemius muscle			
	Fat mass %		Leptin		IL-6		Leptin		IL-6	
Gastrocnemius	*R*	*P*	*R*	*P*	*R*	*P*	*R*	*P*	*R*	*P*
MyoD	**−0.729**	**0.001**	**−0.747**	**0.001**	**−0.708**	**0.001**	**−0.618**	**0.006**	0.427	0.051
MyoG	−0.279	0.147	−0.053	0.424	−0.030	0.454	−0.053	0.424	0.009	0.489
β-Actin	−0.415	0.056	**−0.788**	**0.000**	**−0.720**	**0.001**	**−0.435**	**0.047**	0.271	0.155
Titin	**−0.5357**	**0.0396**	−0.4107	0.1283	**−0.6452**	**0.0094**	−0.3429	0.2109	0.1679	0.5499
IGF-II	**−0.577**	**0.011**	**−0.744**	**0.001**	**−0.664**	**0.003**	**−0.588**	**0.009**	**0.453**	**0.040**
IGFBP-5	**−0.6264**	**0.0165**	**−0.6791**	**0.0076**	**−0.6865**	**0.0067**	−0.5121	0.0612	0.4549	0.1022
PGC-1α	0.068	0.410	0.152	0.303	0.213	0.230	0.020	0.476	0.160	0.292
PGC-1β	−0.350	0.101	**−0.646**	**0.006**	**−0.459**	**0.042**	−0.332	0.113	0.418	0.061

The mice used were 20 weeks old (n = 16). Significant correlations appear in boldface.

(Akt/mammalian target of rapamycin/p70S6) that mediates hypertrophy in skeletal muscle (21). Importantly, the short-term activation by IGF-II/IGFBP-5 of this pathway, in particular Akt phosphorylation, was altered in myotubes exposed to obese VAT adipocytes, which could be responsible for the observed muscle cell atrophy phenotype. This is supported by the observations that long-term treatment by IGF-II and IGFBP-5 was able to correct the muscle atrophy phenotype and restore titin and myosin heavy chain production in the cocultured myotubes while having a minor influence on myotube phenotype alone under control conditions.

Finally, the pathophysiological relevance of our results was further supported in a rodent model of nutritionally induced obesity. Obese mice displayed abnormal distribution of cross-sectional muscle fiber size, adipocyte accumulation, and decreased muscle marker expression.

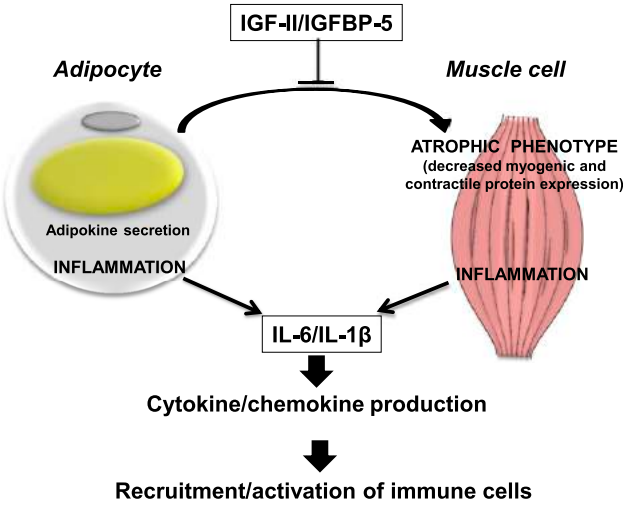

Figure 6—Scheme representing the proposed cross talk between obese adipocytes and muscle cells, which could trigger inflammation and muscle dysfunctions.

Interestingly, the expression of the muscle markers (i.e., MyoD, β-actin, titin, IGF-II, and IGFBP-5) was negatively correlated with inflammation and epididymal fat expansion. We cannot exclude from our in vivo model an additional role of the liver in promoting muscle dysfunction. According to the "portal hypothesis," the liver is directly exposed to VAT-derived factor, which may induce inflammation, then causing skeletal muscle defects such as insulin resistance (46). Moreover, correlative observations made in skeletal muscle need further studies to firmly establish a potential role of intermuscular adipocytes in muscle dysfunction. Several clinical studies (13,31,47) suggest that muscle-derived adipocytes through the secretion of bioactive factors could play a role in muscle deterioration by inducing insulin resistance and negatively affecting myogenesis and muscle performance. Moreover, a recent report (48) showed a potential link between obesity-induced lipotoxicity and muscle insulin resistance through the disruption of 4E-BP1 phosphorylation and protein synthesis. Consequently, a future goal will be to compare both VAT and intermuscular adipocyte phenotypes; the latter still remains unknown.

To conclude, we provide evidence for cross talk between human obese adipocytes and muscle cells leading to muscle atrophy (Fig. 6). The subset of underexpressed muscle-specific genes could constitute a molecular signature of muscle damage induced by hypertrophy of obese WAT. The identification of negative (IL-6/IL-1β) and beneficial (IGF-II/IGFBP-5) molecular actors involved in these dysfunctions opens new avenues for therapeutic strategies of myopathies associated with metabolic disorders.

Acknowledgments. The authors thank Dr. Peter Van Der Ven (Institute for Cell Biology, Bonn, Germany) for providing the anti-human titin monoclonal antibody. The authors also thank the patients and the physician Dr. Christine Poitou of the Nutrition Department of Pitié-Salpétrière Hospital (Paris, France) for patient recruitment. In addition, the authors thank Christophe Klein from the imaging facilities of Centre de Recherche des Cordeliers. For cellular studies,

ethical authorization was obtained from Comités de Protection des Personnes Pitié-Salpêtrière.

Funding. This work was supported by a grant from the European Community Seventh Framework Programme, the Adipokines as Drugs to Combat Adverse Effects of Excess Adipose Tissue project (contract no. HEALTH-FP2-2008-201100), Assistance Publique Hôpitaux de Paris Clinical Research Contract, Emergence Program, University Pierre et Marie Curie (to V.P.), Région Ile de France (FUI-OSEO Sarcob), Fondation pour la Recherche Médicale (grant DEQ20120323701 to K.C.), as well as the French National Agency of Research (French government grant, Investments for the Future," grant no. ANR-10-IAHU, ANR AdipoFib). This work was also supported by the European Community Seventh Framework Programme project MYOAGE (contract HEALTH-F2-2009-223576), the Agence Nationale de la Recherche Genopath-INAFIB (Inflammation, Atrophy and Fibrosis), the Agence Francaise de Lutte contre le Dopage, the CNRS, and the Association Française contre les Myopathies. S.R.-C. and A.V.-P. are supported by Medical Research Council and British Heart Foundation programme grants. Human adipose tissue samples were obtained thanks to Clinical Research Contract Assistance Publique/Direction de la Recherche Clinique grant AOR 02076.

Duality of Interest. No potential conflicts of interest relevant to this article were reported.

Author Contributions. V.P., S.R.-C., and D.L. conceived and performed the experiments, analyzed the data, and wrote the manuscript with the input of all the coauthors. C.R. performed and analyzed multiplex and PCR array experiments. V.A. and F.E.-V. performed the muscle cell culture. A.V.-P. and G.S.B.-B. wrote the manuscript with the input of all the coauthors. K.C. contributed to the clinical investigation and patient recruitment, and wrote the manuscript with the input of all the coauthors. G.S.B.-B. and D.L. are the guarantors of this work and, as such, had full access to all the data in the study and take responsibility for the integrity of the data and the accuracy of the data analysis.

References

1. Cancello R, Tordjman J, Poitou C, et al. Increased infiltration of macrophages in omental adipose tissue is associated with marked hepatic lesions in morbid human obesity. Diabetes 2006;55:1554–1561
2. Villaret A, Galitzky J, Decaunes P, et al. Adipose tissue endothelial cells from obese human subjects: differences among depots in angiogenic, metabolic, and inflammatory gene expression and cellular senescence. Diabetes 2010;59:2755–2763
3. Jensen MD. Role of body fat distribution and the metabolic complications of obesity. J Clin Endocrinol Metab 2008;93(Suppl. 1):S57–S63
4. Harwood HJ Jr. The adipocyte as an endocrine organ in the regulation of metabolic homeostasis. Neuropharmacology 2012;63:57–75
5. Rytka JM, Wueest S, Schoenle EJ, Konrad D. The portal theory supported by venous drainage-selective fat transplantation. Diabetes 2011;60:56–63
6. Fontana L, Eagon JC, Trujillo ME, Scherer PE, Klein S. Visceral fat adipokine secretion is associated with systemic inflammation in obese humans. Diabetes 2007;56:1010–1013
7. Kewalramani G, Bilan PJ, Klip A. Muscle insulin resistance: assault by lipids, cytokines and local macrophages. Curr Opin Clin Nutr Metab Care 2010;13:382–390
8. Akhmedov D, Berdeaux R. The effects of obesity on skeletal muscle regeneration. Front Physiol 2013;4:371
9. Masgrau A, Mishellany-Dutour A, Murakami H, et al. Time-course changes of muscle protein synthesis associated with obesity-induced lipotoxicity. J Physiol 2012;590:5199–5210
10. Boettcher M, Machann J, Stefan N, et al. Intermuscular adipose tissue (IMAT): association with other adipose tissue compartments and insulin sensitivity. J Magn Reson Imaging 2009;29:1340–1345
11. Thomas EL, Saeed N, Hajnal JV, et al. Magnetic resonance imaging of total body fat. J Appl Physiol (1985) 1998;85:1778–1785
12. Gallagher D, Kelley DE, Yim J-E, et al.; MRI Ancillary Study Group of the Look AHEAD Research Group. Adipose tissue distribution is different in type 2 diabetes. Am J Clin Nutr 2009;89:807–814
13. Goodpaster BH, Krishnaswami S, Harris TB, et al. Obesity, regional body fat distribution, and the metabolic syndrome in older men and women. Arch Intern Med 2005;165:777–783
14. Coen PM, Hames KC, Leachman EM, et al. Reduced skeletal muscle oxidative capacity and elevated ceramide but not diacylglycerol content in severe obesity. Obesity (Silver Spring) 2013;21:2362–2371
15. Kemp JG, Blazev R, Stephenson DG, Stephenson GMM. Morphological and biochemical alterations of skeletal muscles from the genetically obese (ob/ob) mouse. Int J Obes (Lond) 2009;33:831–841
16. Denies MS, Johnson J, Maliphol AB, et al. Diet-induced obesity alters skeletal muscle fiber types of male but not female mice. Physiol Rep 2014;2:e00204
17. Borst SE, Conover CF, Bagby GJ. Association of resistin with visceral fat and muscle insulin resistance. Cytokine 2005;32:39–44
18. Vu V, Kim W, Fang X, Liu Y-T, Xu A, Sweeney G. Coculture with primary visceral rat adipocytes from control but not streptozotocin-induced diabetic animals increases glucose uptake in rat skeletal muscle cells: role of adiponectin. Endocrinology 2007;148:4411–4419
19. Dietze D, Koenen M, Röhrig K, Horikoshi H, Hauner H, Eckel J. Impairment of insulin signaling in human skeletal muscle cells by co-culture with human adipocytes. Diabetes 2002;51:2369–2376
20. Kovalik J-P, Slentz D, Stevens RD, et al. Metabolic remodeling of human skeletal myocytes by cocultured adipocytes depends on the lipolytic state of the system. Diabetes 2011;60:1882–1893
21. Glass DJ. PI3 kinase regulation of skeletal muscle hypertrophy and atrophy. Curr Top Microbiol Immunol 2010;346:267–278
22. Pedersen BK, Febbraio MA. Muscles, exercise and obesity: skeletal muscle as a secretory organ. Nat Rev Endocrinol 2012;8:457–465
23. Whittle AJ, Carobbio S, Martins L, et al. BMP8B increases brown adipose tissue thermogenesis through both central and peripheral actions. Cell 2012;149:871–885
24. Riehle C, Wende AR, Zaha VG, et al. PGC-1β deficiency accelerates the transition to heart failure in pressure overload hypertrophy. Circ Res 2011;109:783–793
25. Briguet A, Courdier-Fruh I, Foster M, Meier T, Magyar JP. Histological parameters for the quantitative assessment of muscular dystrophy in the mdx-mouse. Neuromuscul Disord 2004;14:675–682
26. Pellegrinelli V, Rouault C, Veyrie N, Clément K, Lacasa D. Endothelial cells from visceral adipose tissue disrupt adipocyte functions in a three-dimensional setting: partial rescue by angiopoietin-1. Diabetes 2014;63:535–549
27. Pellegrinelli V, Heuvingh J, du Roure O, et al. Human adipocyte function is impacted by mechanical cues. J Pathol 2014;233:183–195
28. Decary S, Mouly V, Hamida CB, Sautet A, Barbet JP, Butler-Browne GS. Replicative potential and telomere length in human skeletal muscle: implications for satellite cell-mediated gene therapy. Hum Gene Ther 1997;8:1429–1438
29. Delaporte C, Dautreaux B, Fardeau M. Human myotube differentiation in vitro in different culture conditions. Biol Cell 1986;57:17–22
30. Rouault C, Pellegrinelli V, Schilch R, et al. Roles of chemokine ligand-2 (CXCL2) and neutrophils in influencing endothelial cell function and inflammation of human adipose tissue. Endocrinology 2013;154:1069–1079
31. Hilton TN, Tuttle LJ, Bohnert KL, Mueller MJ, Sinacore DR. Excessive adipose tissue infiltration in skeletal muscle in individuals with obesity, diabetes mellitus, and peripheral neuropathy: association with performance and function. Phys Ther 2008;88:1336–1344
32. Dalmas E, Rouault C, Abdennour M, et al. Variations in circulating inflammatory factors are related to changes in calorie and carbohydrate intakes early in the course of surgery-induced weight reduction. Am J Clin Nutr 2011;94:450–458
33. Spranger J, Kroke A, Möhlig M, et al. Inflammatory cytokines and the risk to develop type 2 diabetes: results of the prospective population-based European Prospective Investigation into Cancer and Nutrition (EPIC)-Potsdam Study. Diabetes 2003;52:812–817

34. Stapp JM, Sjoelund V, Lassiter HA, Feldhoff RC, Feldhoff PW. Recombinant rat IL-1beta and IL-6 synergistically enhance C3 mRNA levels and complement component C3 secretion by H-35 rat hepatoma cells. Cytokine 2005;30:78–85

35. Ren H, Yin P, Duan C. IGFBP-5 regulates muscle cell differentiation by binding to IGF-II and switching on the IGF-II auto-regulation loop. J Cell Biol 2008; 182:979–991

36. Glass DJ. Skeletal muscle hypertrophy and atrophy signaling pathways. Int J Biochem Cell Biol 2005;37:1974–1984

37. Chau Y-Y, Bandiera R, Serrels A, et al. Visceral and subcutaneous fat have different origins and evidence supports a mesothelial source. Nat Cell Biol 2014; 16:367–375

38. Macotela Y, Emanuelli B, Mori MA, et al. Intrinsic differences in adipocyte precursor cells from different white fat depots. Diabetes 2012;61:1691–1699

39. Yu J, Shi L, Wang H, et al. Conditioned medium from hypoxia-treated adipocytes renders muscle cells insulin resistant. Eur J Cell Biol 2011;90: 1000–1015

40. Kern PA, Ranganathan S, Li C, Wood L, Ranganathan G. Adipose tissue tumor necrosis factor and interleukin-6 expression in human obesity and insulin resistance. Am J Physiol Endocrinol Metab 2001;280:E745–E751

41. Moschen AR, Molnar C, Enrich B, Geiger S, Ebenbichler CF, Tilg H. Adipose and liver expression of interleukin (IL)-1 family members in morbid obesity and effects of weight loss. Mol Med 2011;17:840–845

42. Buxboim A, Ivanovska IL, Discher DE. Matrix elasticity, cytoskeletal forces and physics of the nucleus: how deeply do cells 'feel' outside and in? J Cell Sci 2010;123:297–308

43. Berkes CA, Tapscott SJ. MyoD and the transcriptional control of myogenesis. Semin Cell Dev Biol 2005;16:585–595

44. Le Grand F, Rudnicki MA. Skeletal muscle satellite cells and adult myogenesis. Curr Opin Cell Biol 2007;19:628–633

45. Gautel M. Cytoskeletal protein kinases: titin and its relations in mechanosensing. Pflugers Arch 2011;462:119–134

46. Cai D, Yuan M, Frantz DF, et al. Local and systemic insulin resistance resulting from hepatic activation of IKK-beta and NF-kappaB. Nat Med 2005;11: 183–190

47. Takegahara Y, Yamanouchi K, Nakamura K, Nakano S, Nishihara M. Myotube formation is affected by adipogenic lineage cells in a cell-to-cell contact-independent manner. Exp Cell Res 2014;324:105–114

48. Stephens FB, Chee C, Wall BT, et al. Lipid induced insulin resistance is associated with an impaired skeletal muscle protein synthetic response to amino acid ingestion in healthy young men. Diabetes. 18 December 2014 [Epub ahead of print]